Journal of Electroanalytical Chemistry 742 (2015) 54–61

Contents lists available at ScienceDirect

Journal of Electroanalytical Chemistry

journal homepage: www.elsevier.com/locate/jelechem

Direct electrochemical oxidation of Abelson tyrosine-protein kinase 1 and evaluation of its interaction with synthetic substrate, ATP and inhibitors

Oana M. Popa [a,b], Victor C. Diculescu [a,*]

[a] Departamento de Engenharia Mecânica, Faculdade de Ciências e Tecnologia, Universidade de Coimbra, Rua Luís Reis Santos, 3030-788 Coimbra, Portugal
[b] Faculty of Physics, University of Bucharest, 077125 Magurele-Bucharest, Romania

ARTICLE INFO

Article history:
Received 8 October 2014
Received in revised form 19 January 2015
Accepted 22 January 2015
Available online 11 February 2015

Keywords:
Abelson tyrosine-protein kinase 1 (ABL1)
Protein
Electrochemistry
Oxidation
Interaction
Inhibitors

ABSTRACT

The electrochemical behaviour of Abelson protein-tyrosine kinase 1 (ABL1) and its interaction with synthetic substrate abltide EAIYAAPFAKKK, ATP, and inhibitors genistein, imatinib mesylate and danusertib were studied by differential pulse voltammetry using a glassy carbon electrode. In neutral electrolytes one oxidation peak due to histidine residues was observed. In acid and basic media the enzyme undergoes conformational modifications which lead to exposure of more electroactive amino acid to the electrode surface facilitating their oxidation. The interaction of ABL1 with the synthetic substrate involves the coiling of abltide around the enzyme which suppresses the oxidation of abltide tyrosine residue and leads the exposure of ABL1 electroactive amino acids to the electrode surface and occurrence of new electrochemical signals. The binding of ATP and ATP-competitive synthetic inhibitors imatinib mesylate, and danusertib results in stable complexes that maintains the symmetry of the enzyme but the electroactive centres of the compounds are hidden inside the binding site, preventing their oxidation. The natural inhibitor genistein is encountered on the outer surface of the enzyme and the electroactive centres are available for oxidation.

1. Introduction

Protein kinases catalyse the transfer of the γ-phosphate group of ATP to specific amino acids on protein substrates. Phosphorylation processes by kinases regulate important intra- and inter-cellular function with direct influence on cellular metabolism, growth and proliferation [1]. Any dysregulation in the finely-tuned phosphorylation mechanism is associated with anomalies [2], and a variety of dysfunctional kinases has been described in tumours [3]. The most prominent example is the constitutively activated Abelson tyrosine-protein kinase 1 (ABL1), the biomarker of chronic myeloid leukaemia (CML) [4]. Since its discovery, this oncoprotein became target for drug development for CML treatment [5].

Crystallography was used throughout the drug discovery process and to obtain diverse information essential for structure-based drug design [6]. The understanding of kinase structure was shown to be a critical issue for the development of inhibitors [7]. The protein kinase (catalytic) domain is highly conserved, Scheme 1, and presents two units denoted as N- and C-terminal lobes [8]. The binding site for ATP is situated between the two lobes in proximity to the substrate binding site on the C-lobe. An important regulatory element is the activation loop [7], which adopts an open conformation that allows access to the substrate binding site, while the highly conserved aspartate-phenylalanine-glycine (DFG) motif [9] located at its N-terminal end is oriented toward the γ-phosphate group of ATP.

In the search for kinases inhibitors, flavonoids such as genistein, Scheme 2A, have been initially described but with limited efficacy [10,11]. The research in finding inhibitors has been then extended to ATP-competitive synthetic ligands and led to imatinib mesylate, Scheme 2B, which revolutionised drug therapy of CML [12,13]. Recent compounds such as danusertib, Scheme 2C, simultaneously target different kinases including imatinib-resistant mutants [14,15], being effective in multiple preclinical tumour models [16].

The crystallographic analysis on protein kinases with inhibitors and synthetic substrate peptide sequences usually used for activity assays has shown the occurrence of conformational modifications upon ligand binding [17] which in turn alters the enzymes correct functioning. Thus, simple, adaptable and label-free techniques rep-

* Corresponding author at: Instituto Pedro Nunes, Laboratório de Electroanálise e Corrosão, Rua Pedro Nunes, 3030-199 Coimbra, Portugal. Tel./fax: +351 239 700 943/912.
E-mail address: victorcd@ipn.pt (V.C. Diculescu).

http://dx.doi.org/10.1016/j.jelechem.2015.01.035
1572-6657/

resent necessary alternatives for fast assessment of proteins conformational modifications upon ligands binding.

Electrochemical techniques in proteomics have been largely applied in sensor technology [18–20] and for the study of proteins or protein domains containing centres with fast-reversible redox reactions [21]. Nevertheless, the voltammetric methods have the ability to detect protein conformational changes [22–24] through the variation of the oxidation peaks of electroactive amino acids tyrosine, tryptophan, histidine, cysteine and methionine [25–28].

The present study deals with the electrochemical characterisation of the ABL1 tyrosine kinase and its interaction with synthetic substrate peptide EAIYAAPFAKKK, ATP and inhibitors genistein, imatinib mesylate, and danusertib, Scheme 2, which electrochemical behaviours have been previously studied [29–32]. The electrochemical investigation of ABL1 electron-transfer reactions before and after interaction with substrates and inhibitors allows detection of proteins conformational modifications upon interaction with ligands, a qualitative understanding of the interaction mechanisms and contributes to the development of structure–activity relationships in ligand-ABL1 kinase interactions.

2. Experimental

2.1. Materials and reagents

Abelson tyrosine-protein kinase 1 (ABL1) and ATP from Sigma–Aldrich, ABL1 synthetic substrate peptide abltide (EAIYAAPFAKKK) from Enzo Life Sciences, imatinib mesylate from Novartis-Portugal, genistein and danusertib from Selleck Chemicals, were used without purification.

The 0.1 M ionic strength supporting electrolyte solutions: acetate buffer pH 3.4–5.6, phosphate buffer pH 5.7–8.0, NaOH/$Na_2B_2O_7$ pH 9.1–10.0, were prepared using analytical grade reagents and purified water from a Millipore Milli-Q system (conductivity $\leqslant$ 0.1 μS cm^{-1}). Stock solutions of 10 μg mL^{-1} ABL1, 100 μM ATP and 300 μM abltide were prepared in pure water. 100 μM imatinib mesylate, 1 mM genistein and danusertib were prepared in ethanol/deionised water mixtures of 10/90, v/v. All stock solutions were kept at +4 °C until further utilisation. Solutions of different concentrations of ABL1, abltide, ATP, genistein, imatinib mesylate and danusertib were obtained by dilution of the appropriate volume in supporting electrolyte.

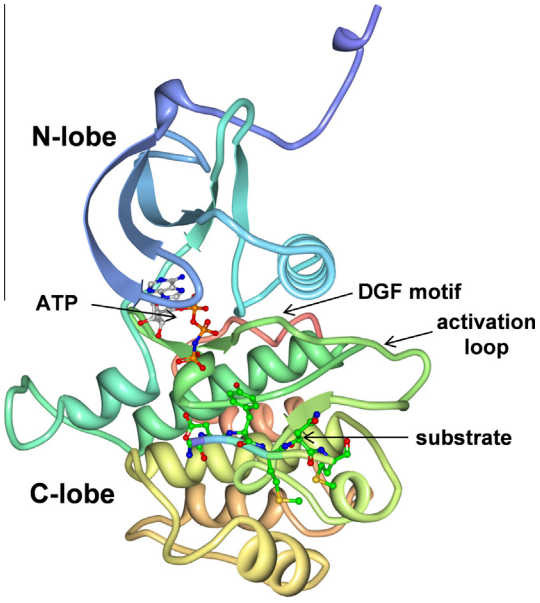

Scheme 1. Structure of insulin receptor tyrosine kinase in complex with peptide substrate and ATP (structure PDB ID: 1IR3 [8]).

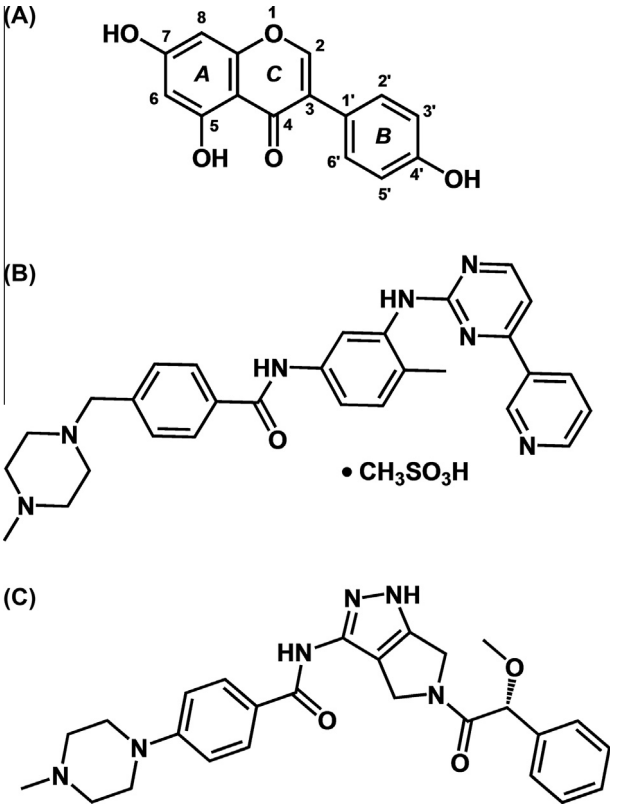

Scheme 2. Chemical structure of: (A) genistein, (B) imatinib mesylate and (C) danusertib.

Microvolumes were measured using EP-10 and EP-100 Plus Motorized Microliter Pippettes (Rainin Instrument Co., Inc., Woburn, USA). The pH measurements were carried out with a Crison microph 2001 pH-meter with an Ingold combined glass electrode. All experiments were done at room temperature (25 ± 1 °C).

2.2. Voltammetric parameters and electrochemical cells

Voltammetric experiments were carried out using a CompactStat.e running with IviumSoft 2.124, Ivium Technologies, The Netherlands. The measurements were carried out in the presence of dissolved atmospheric oxygen using a three-electrode system in a 0.5 mL one-compartment electrochemical cell. A glassy carbon (GCE, d = 1.0 mm), a Pt wire, and a Ag/AgCl (3 M KCl) were used as working, auxiliary and reference electrodes, respectively.

The experimental conditions for differential pulse voltammetry (DPV) were: pulse amplitude of 50 mV, pulse width of 100 ms, step potential 2 mV and scan rate of 5 mV s^{-1}.

The GCE was polished using diamond spray, particle size 3 μm (Kemet, UK) before each electrochemical experiment. After polishing, it was rinsed thoroughly with Milli-Q water. Following this mechanical treatment, the GCE was placed in buffer supporting electrolyte and differential pulse voltammograms were recorded until a steady state baseline voltammogram was obtained. This procedure ensured very reproducible experimental results.

2.3. Incubation procedure and control experiments

The interaction of ABL1 with abltide, ATP, genistein, imatinib and danusertib was studied *in* incubated solutions in buffer electrolytes by mixing the desired quantities of reagents. The

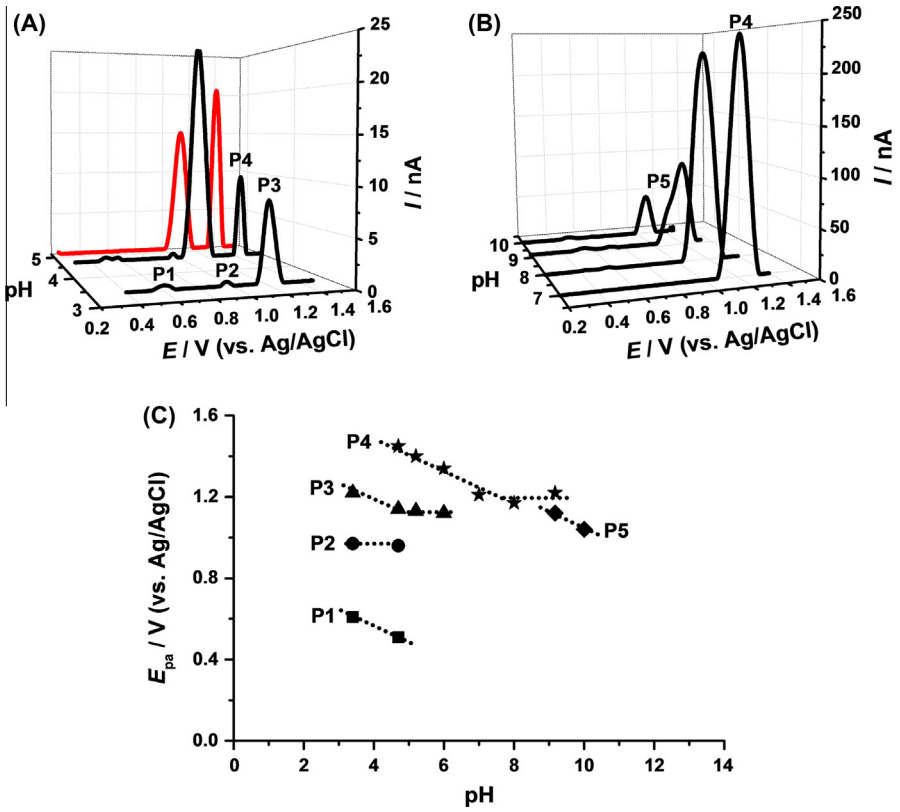

Fig. 1. DP voltammograms recorded in solutions of 1 μg mL^{-1} ABL1 in: (A) acid and (B) neutral and alkaline electrolytes; (C) graph of E_{pa} of ABL1 oxidation peaks vs. pH.

concentrations were selected so that the oxidation currents of enzyme and substrate/inhibitor were comparable upon interaction and in the same range as those used in electrochemical assays for detection of ABL1 activity and inhibition [20]. The differential pulse (DP) voltammograms were recorded after different incubation times. Between measurements the GCE surface was always cleaned in order to avoid the adsorption of oxidation products which can reduce the electroactive area.

For control experiments, distinct solutions of ABL1, abltide, ATP, genistein, imatinib or danusertib were individually prepared, stored and analysed in similar conditions and during the same time periods as the incubated solutions.

The thermal denaturation of ABL1 was carried out by incubation at 90 ± 3 °C during different periods of time in electrolytes with pH values of 3.4 and 7.0. Then, the solution was immediately cooled at room temperature and analysed by differential pulse voltammetry.

2.4. Acquisition and presentation of data

All voltammograms presented were smoothed and baseline-corrected using an automatic function included in the IviumSoft version 2.124 [32].

ChemDraw Ultra 8.0 implemented into ChemOffice 2004 software from CambridgeSoft Corporation was used for the presentation of all chemical structures.

Origin Pro 9.0 SR2 from OriginLab Corporation was used for the presentation of all the experimental data reported in this work.

The hydropathicity plots [33] of ABL1, sequence P00519 provided by UniProtKB/Swiss-Prot [34], were obtained using the online tool ProtScale from ExPASy – Bioinformatic Resource Portal [35] with a window size of 9 amino acids.

The enzymes structures presented were obtained using the Protein Workshop 4.1.0 [36] software from Protein Data Bank RCSB PDB [37,38].

3. Results and discussion

3.1. Voltammetric characterisation of ABL1

The voltammetric behaviour of ABL1 has been investigated at a glassy carbon electrode (GCE) by differential pulse (DP) voltammetry. DP voltammograms were recorded in freshly prepared solutions of 1.0 μg mL^{-1} ABL1 in electrolytes with pH values between 3.4 and 10.0.

The voltammogram in pH = 3.4 showed three consecutive charge transfer reactions at peaks P1, P2, and P3, Fig. 1A and C. For pH = 4.3, a new peak P4 occurred at more positive potential values, Fig. 1A and C. Increasing the pH of the supporting electrolyte, peaks P1, P2 and P3 currents progressively decreased and disappeared for pH > 6.0, Fig. 1A and B. For 6.0 < pH < 8.0 only peak P4 appeared with constant current values, Fig. 1B and C. For pH > 9.0, peak P4 decreased and broadened so that a new charge transfer reaction at peak P5 occurred at less positive potential values. At pH = 10.0, peak P5 was the only reaction observed.

The effect of thermal denaturation of ABL1 was investigated in solutions of 1.0 μg mL^{-1} ABL1 in electrolytes with pH 3.4 and 7.0. At pH = 3.4, Fig. 2A, the DP voltammogram recorded in the denatured solution maintained the profile of the voltammogram in the freshly prepared solution. Contrary, at pH = 7.0, Fig. 2B, the DP voltammogram in the denatured solution showed the decrease of ABL1 oxidation peak and the occurrence of new electrochemical signals at lower positive potential values.

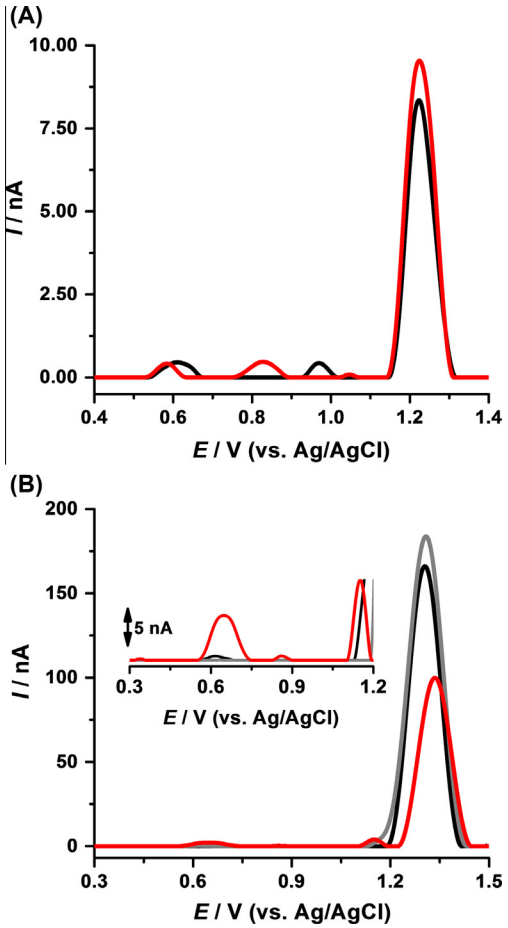

Fig. 2. DP voltammograms recorded in solutions of 1 μg mL^{-1} ABL1 in: (A) pH = 3.4 and (B) pH = 7.0; (black curve) before and after (red curve) thermal denaturation or (grey curve) 48 h incubation in buffer. (For interpretation of the references to colour in this figure legend, the reader is referred to the web version of this article.)

Also, the stability of ABL1 in pH = 7.0 0.1 M phosphate buffer electrolyte was tested, Fig. 2B. The DP voltammogram recorded after different incubation times did not show any modification of the ABL1 oxidation peak or the occurrence of new electrochemical signals.

In order to identify the origin of the oxidation peaks of ABL1, the primary structure of ABL1 tyrosine kinase [34] has been analysed. Among 1130 amino acids, 100 residues are electroactive [25–27]. 31 residues of tyrosine, 13 of tryptophan, 24 of histidine, 14 of cysteine and 18 of methionine were identified, Table 1. Besides, the active conformation of ABL1 contains 12 tyrosine residues than may be phosphorylated leading to phosphotyrosine which is also electroactive [28]. All these amino acids are randomly distributed along the polypeptide chain.

Table 1
Oxidation potentials (vs. Ag/AgCl) of electroactive amino acids at pH = 4.5 0.1 M acetate and pH = 7.0 0.1 M phosphate buffers.

	pH = 4.5			pH = 7.0		
	E_p1_a/V	E_p2_a/V	E_p3_a/V	E_p1_a/V	E_p2_a/V	E_p3_a/V
Tyrosine	0.79	–	–	0.63	–	–
Phosphotyrosine	1.37			1.37		
Tryptophan	0.76	1.11	–	0.63	1.08	–
Histidine	1.35	–	–	1.15	–	–
Cysteine	0.70	0.88	1.35	0.52	0.88	1.27
Methionine	1.05	1.25	–	–	1.25	–

The interaction of proteins with electrodes is directly influenced by surface properties. In general, the GCE surface is hydrophobic favouring interaction with hydrophobic protein domains. The Kyte–Doolittle hydropathy scale is used for the identification of the hydrophobicity and/or polarity of a protein or protein sequence [33,34]. The Kyte–Doolittle plot for the ABL1, Fig. 3A, showed a general hydrophilic character with intercalated hydrophobic sequences. Most of the electroactive amino acids are incorporated into the hydrophilic regions, and contained into the kinase domain of the ABL1, Fig. 3B.

In these conditions, the voltammetric behaviour of ABL1 is explained considering the pH effect on the secondary and tertiary protein structure in which the amino acids are organised according to their polarity/hydrophobicity.

For electrolytes with 6.0 < pH < 8.0, the protein is in the native conformation. The enzyme conformation is stable since no modification of the voltammetric profile was observed after 48 h of incubation in buffer, but can be destabilised by thermal denaturation, Fig. 2B. Thus, for 6.0 < pH < 8.0, the enzyme adopts a compact rigid structure that hinders the interaction of most electroactive amino acids with the GCE surface and therefore their oxidation. Considering the potential values in Table 1, the peak recorded in solutions of ABL1 in electrolytes with 6.0 < pH < 8.0, Figs. 1B and 2B, is due to the oxidation of histidine residues.

For pH < 6.0, the native protein structure is destabilised and the voltammetric profile in freshly prepared solutions is similar to that recorded after thermal denaturation in the same conditions, Figs. 1A and 2A. Thus, for pH < 6.0, ABL1 undergoes conformational modifications which involve exposure of other electroactive residues to the electrode surface facilitating their oxidation, Fig. 1A.

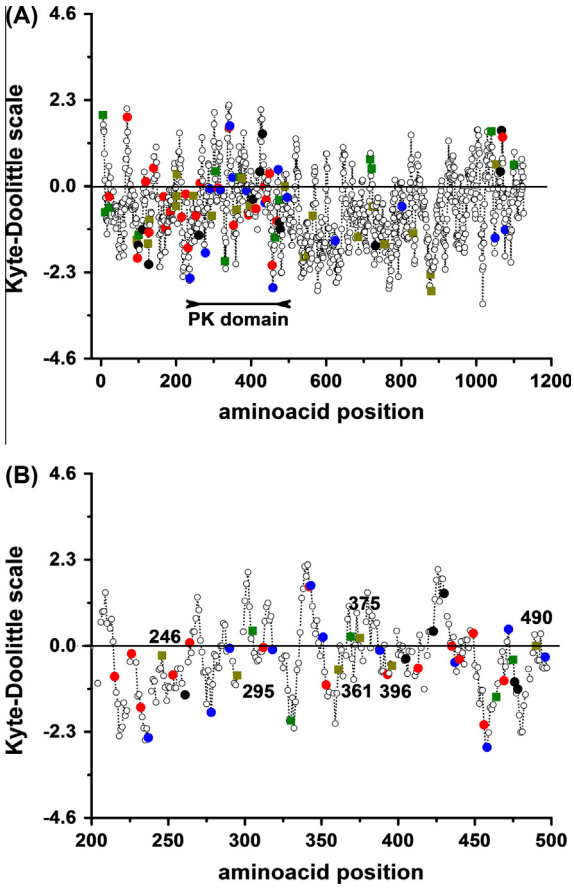

Fig. 3. Hydropathicity plot of the amino acid sequence of: (A) ABL1 and (B) ABL1 kinase domain. Highlighted electroactive aminoacids residues: (●) tyrosine, (●) tryptophan, (■) histidine, (■) cysteine and (●) methionine.

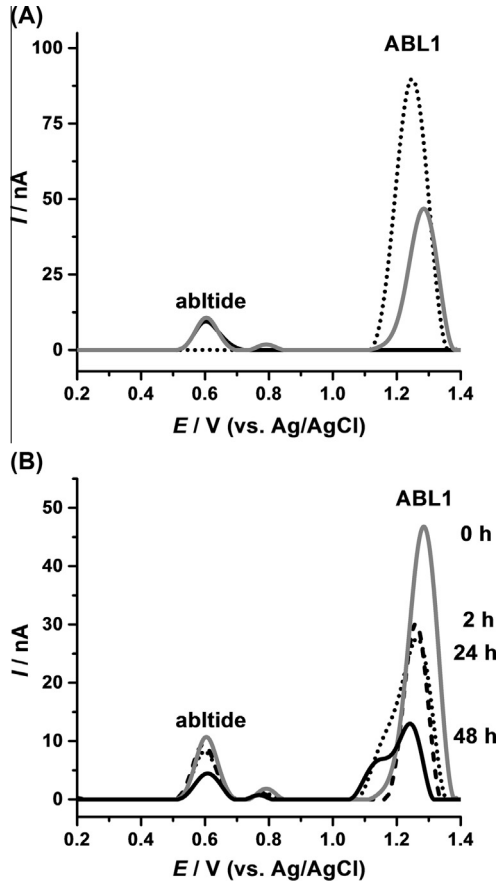

Fig. 4. DP voltammograms base-line corrected in solutions of: (A) (black curve) 5 μM abltide, (dotted curve) 0.5 μg mL^{-1} ABL1 before and (grey curve) after 0 h incubation, and (B) after different incubation times, in pH = 7.0.

The oxidation peaks observed at lower potential values in acid media are due to charge transfer reactions of tyrosine and tryptophan, Table 1.

3.2. Voltammetric characterisation of ABL1 interaction with substrates

3.2.1. Synthetic substrate abltide (EAIYAAPFAKKK)

The electrochemical behaviour of synthetic substrate abltide EAIYAAPFAKKK was reviewed for peaks identification. The DP voltammogram recorded in a solution of 5 μM abltide in pH = 7.0 0.1 M phosphate buffer showed one peak at E_{pa} = +0.63 V due to the oxidation of tyrosine residue, Fig. 4A. No modification of the abltide oxidation peak was observed upon incubation in buffer.

The DP voltammogram recorded in a solution of 0.5 μg mL^{-1} ABL1 in pH = 7.0 0.1 M phosphate buffer has shown one oxidation peak at E_{pa} = +1.23 V, Fig. 4A.

The interaction between ABL1 and abltide was studied in incubated solutions. DP voltammograms were recorded after different incubation times. Between measurements the GCE surface was always cleaned in order to avoid the adsorption of oxidation products which can reduce the electroactive area.

The DP voltammograms recorded in a mixt solution of 5 μM abltide and 0.5 μg mL^{-1} ABL1 in pH = 7.0 0.1 M phosphate buffer at 0 h incubation time, showed both oxidation peaks of abltide and ABL1, Fig. 4A. The abltide oxidation peak maintained the current whereas the ABL1 decreased and shifted to more positive potential values. Also, a new peak appeared at E_{pa} = +0.79 V, Fig. 4A.

Increasing the incubation time, the ABL1 oxidation peak progressively decreased and reached constant values after 48 h, Fig. 4A. Simultaneously, the peak became broader, and a new electrochemical signal at E_{pa} = +1.14 V increased in a time-dependent manner, Fig. 4B. At the same time, the decrease of the abltide peak current was observed.

The decrease of the abltide oxidation peak with increasing incubation time is explained considering that, upon interaction, the phenol ring of the tyrosine residue on the synthetic substrate is oriented toward the interior of the active site, as previously described [8]. The coiling of the abltide strands around the enzyme leads to structural modifications which are responsible for the decrease of the ABL1 oxidation peak at E_{pa} = +1.23 V, and exposure of other electroactive amino acids at the electrode surface, identified through the occurrence of new electrochemical signals at E_{pa} = +0.79 V and E_{pa} = +1.14 V. The abltide peak observed for longer incubation times was due the oxidation of free, uncoupled abltide strands.

3.2.2. ATP

The interaction between ABL1 and ATP was initially studied in incubated solutions in pH = 7.0 0.1 M phosphate buffer (not shown). In these conditions, the ATP and ABL1 oxidation peaks overlapped turning difficult their visualisation. For this reason, the experiments were carried out in solutions of 50 μM ATP and 1.0 μg mL^{-1} ABL1 in pH = 5.7 0.1 M acetate buffer.

The DP voltammogram recorded at 0 h incubation time showed both ATP and ABL1 oxidation peaks at E_{pa} = +1.23 V and E_{pa} = +1.40 V, respectively, with similar currents as recorded in individual solutions, Fig. 5A.

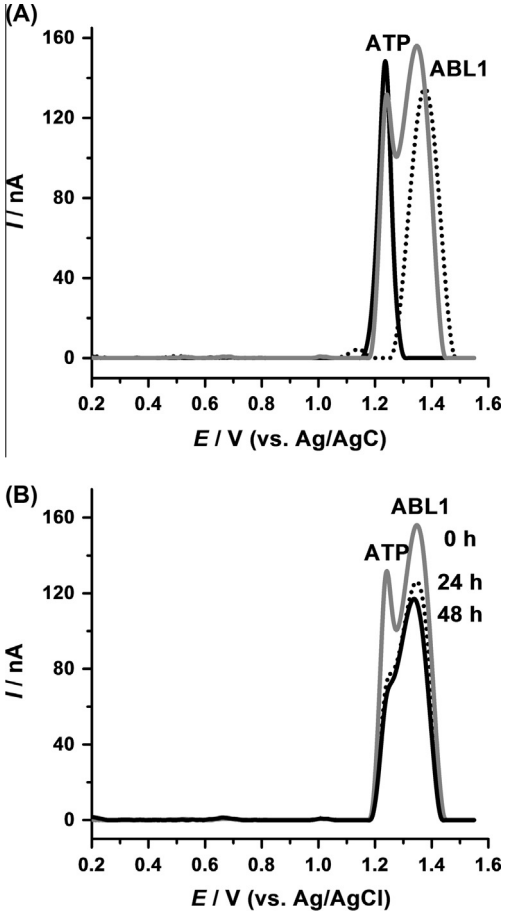

Fig. 5. DP voltammograms base-line corrected in solutions of: (A) (black curve) 50 μM ATP, (dotted curve) 1.0 μg mL^{-1} ABL1 before and (grey curve) after 0 h incubation, and (B) after different incubation times, in pH = 5.7.

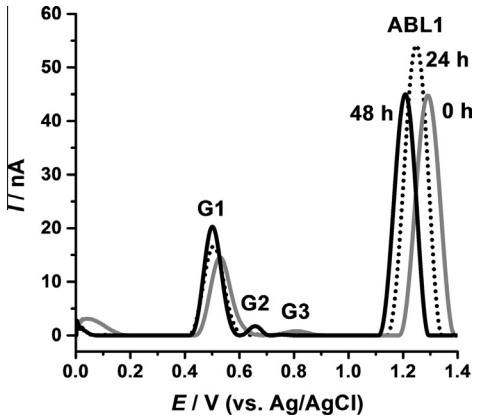

Fig. 6. DP voltammograms base-line corrected in 5 μM genistein incubated during different times with 0.5 μg mL^{-1} ABL1 in pH = 7.0.

DP voltammograms were recorded in the same solution after different incubation periods, always with a clean GCE surface, Fig. 5B. Increasing the incubation time, the ABL1 peak remained constant. The ATP oxidation peak progressively decreased in a time-dependent manner but constant values were reached after 24 h of incubation. No other electrochemical signal was observed. Also, the ATP oxidation peak occurred with the same current and at the same potential value upon incubation in buffer.

The results suggest that the interaction between ABL1 and ATP leads to the formation of stable complex that maintains the symmetry of the enzyme since practically no variation of the ABL1 oxidation peak and/or appearance of new electrochemical signals was observed. The ATP electroactive centres are hidden inside the ATP-binding site, preventing their oxidation. Also, the occurrence of ATP peak for long incubation periods was due the oxidation of free, uncoupled ATP molecules.

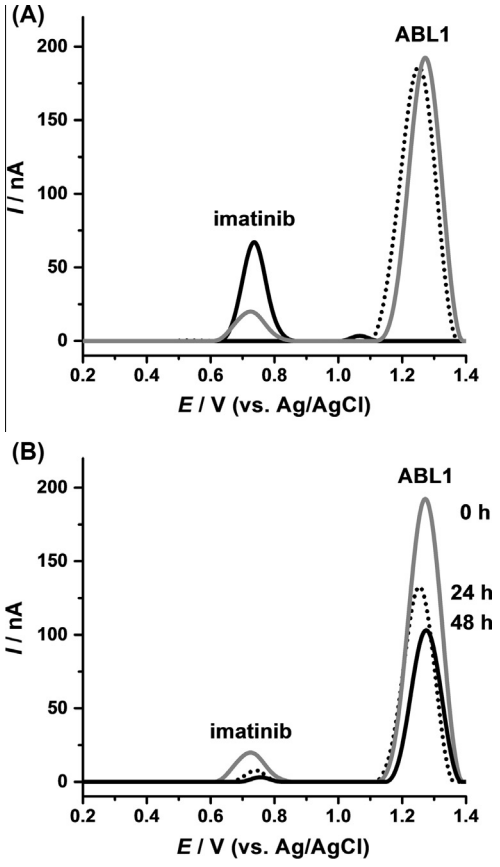

Fig. 7. DP voltammograms base-line corrected in solutions of: (A) (black curve) 5 μM imatinib, (dotted curve) 1.0 μg mL^{-1} ABL1 before and (grey curve) after 0 h incubation, and (B) after different incubation times, in pH = 7.0.

3.3. Voltammetric characterisation of ABL1 interaction with inhibitors

3.3.1. Natural inhibitor genistein

The electrochemical behaviour of genistein was previously characterised [29]. The DP voltammogram (not shown) recorded in a solution of genistein showed three consecutive charge transfer reactions peaks G1, G2 and G3 due to oxidation of the –OH groups at positions C4′, C7 and C5, respectively [29,30].

The interaction between ABL1 and genistein was evaluated in incubated solutions containing 5 μM genistein and 0.5 μg mL^{-1} ABL1 in pH = 7.0 0.1 M phosphate buffer. On the DP voltammogram at 0 h incubation time genistein oxidation peaks G1 and G3 were observed at E_p1_a = +0.53 V and E_p3_a = +0.82 V while the ABL1 peak occurred at E_{pa} = +1.30 V, Fig. 6.

Increasing the incubation time, genistein oxidation peak G1 and ABL1 peak shifted to more negative potential values while peak G3 disappeared. Instead, peak G2 occurred at E_p2_a = +0.67 V. Small fluctuations of the currents were observed either in the case of genistein or ABL1. On the other hand, no modification of genistein oxidation peak was observed upon incubation in buffer.

The behaviour described is in agreement with a two-step interaction mechanism. Initially, genistein binding to ABL1 involves the –OH group at position C7 in ring *A*, which explains the disappearance of genistein peak G2 on the voltammogram recorded at 0 h incubation. The formation of this weak genistein-ABL1 complex occurs through hydrogen bonding, and then is further stabilised through van der Waals and electrostatic interactions.

Although genistein was described as an ATP-competitive kinase inhibitor, it does not bind in the ATP-binding site of the enzyme but to a region close to it [10,11]. In this configuration, genistein is encountered on the outer surface of the enzyme, and the electroactive centres are available for oxidation in agreement with the occurrence of genistein oxidation peaks after long incubation periods. Genistein binding to ABL1 does not induce large enzyme structural modifications but rather alters protein hydrophobicity and consequently its interaction with the electrode surface facilitating the oxidation.

3.3.2. Synthetic inhibitors imatinib mesylate and danusertib

The electrochemical oxidation of imatinib mesylate and danusertib at a glassy carbon electrode [31,32], showed one main

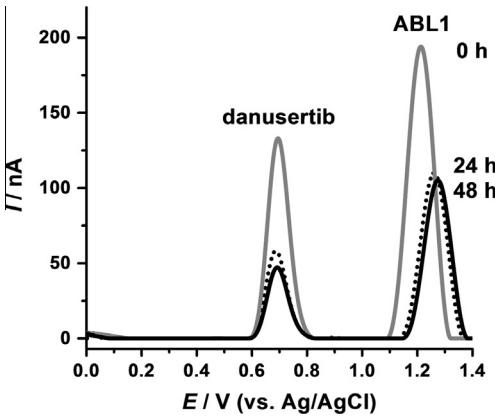

Fig. 8. DP voltammograms base-line corrected in 5 μM danusertib incubated during different times with 1.0 μg mL^{-1} ABL1 in pH = 7.0.

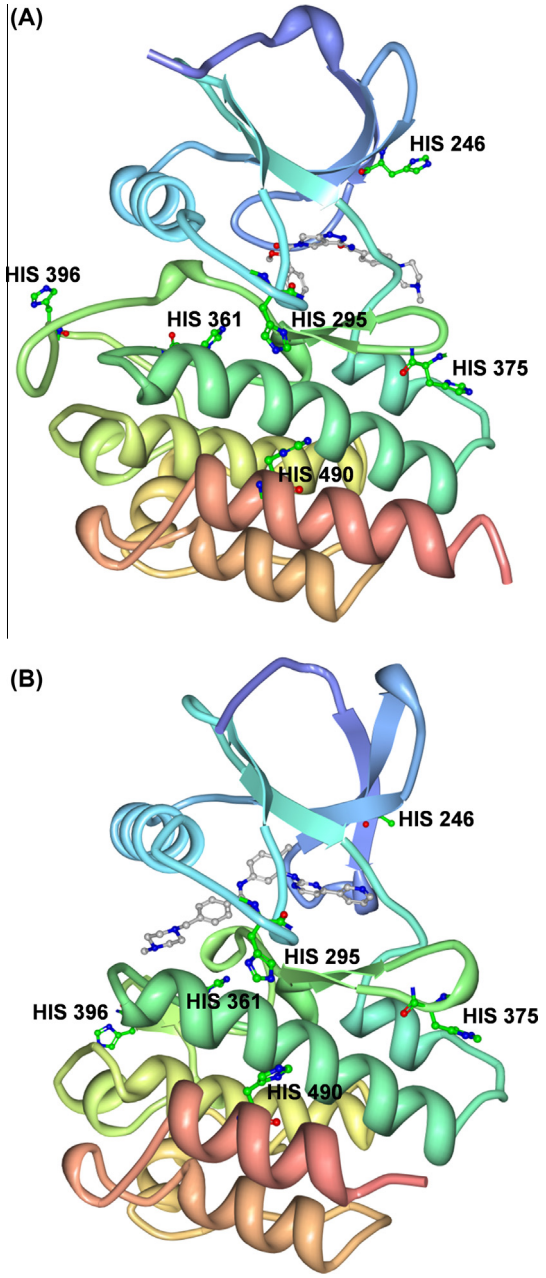

Scheme 3. Structures of ABL1 tyrosine kinase in complex with: (A) danusertib (structure PDB ID: 2V7A [15]) and (B) imatinib mesylate (structure PDB ID: 2HYY [13]).

charge transfer reaction, Figs. 7A and 8, due to the oxidation of the amine moiety. At higher positive potential values small peaks corresponded to piperazine moiety, Fig. 7A.

The interaction between imatinib and ABL1 was studied in incubated solutions containing 5 μM imatinib and 1.0 μg mL^{-1} ABL1 in pH = 7.0 0.1 M phosphate buffer. The DP voltammogram at 0 h incubation showed the peak corresponding to the oxidation of imatinib with a lower current, and the constant ABL1 peak, Fig. 7A.

Increasing the incubation time, a progressive, time-depend decrease of the imatinib oxidation peak was observed and almost disappeared for 48 h of incubation, Fig. 7B. At the same time, the oxidation peak of ABL1 also decreased but reached constant values for longer incubation times.

A similar behaviour was observed for the interaction of danusertib with ABL1, Fig. 8. In this case, danusertib oxidation peak reached constant values after 24 h of incubation. On the other hand, the ABL1 structural modifications are more pronounced and the ABL1 oxidation peak shifted to more positive potential values.

The stability of both compounds in the experimental condition was also investigated, and no modification of the voltammetric profiles was observed after incubation in buffer.

Both imatinib mesylate and danusertib are ATP-competitive inhibitors but, contrary to genistein, their interaction with ABL1 kinase involves the ATP-binding site. Upon interaction, the activation loop adopts different conformations [7,9,13,15], which are responsible for the differences in the observed electrochemical behaviour, Scheme 3. The amino acids sequence of the activation loop presents two electroactive residues: Met 398 and His386. The analysis of the conformations of ABL1 complexes with imatinib and danusertib show a more profound effect on His386. In the case of danusertib-ABL1 complex, Scheme 3A, the His386 residue is flipped apart from the enzyme surface [15] and this configuration is responsible for the higher oxidation potential observed on the voltammograms recorded in incubated solutions of danusertib and ABL1. In the case of imatinib-ABL1 complex, Scheme 3B, the His386 appears closer to enzyme surface [15] facilitating oxidation.

On the other hand, the decrease of both imatinib and danusertib oxidation peaks for long incubation times suggests that their interaction with ABL1 also results in stable complexes in which the inhibitors electroactive centres are hidden inside the ATP-binding site, preventing their oxidation.

4. Conclusion

The electrochemical behaviour of ABL1 protein tyrosine kinase was studied by differential pulse voltammetry using a glassy carbon electrode. In neutral electrolytes, the protein maintain the native, compact and rigid conformation that hinders the interaction of most electroactive amino acids with the GCE surface and therefore their oxidation. One anodic peak current due to the oxidation of histidine residues was observed. In acid and basic media the enzyme native structure is destabilised leading to exposure of electroactive amino acid residues to the electrode surface facilitating their oxidation.

A systematic study of the interaction between ABL1 protein tyrosine kinase and the synthetic substrate abltide EAIYAAPFAKKK, ATP and inhibitors genistein, imatinib mesylate, and danusertib was carried out in incubated solutions. Upon interaction with the enzyme, the tyrosine residue of abltide is oriented toward the interior of the active site becoming unavailable for oxidation. The coiling of the abltide strands around the enzyme leads to the exposure of ABL1 electroactive amino acids to the GCE surface and the occurrence of new electrochemical signals. Contrary, the interaction between ABL1 and ATP results in a stable complex that maintains the symmetry of the enzyme and the ATP electroactive centres are hidden inside the ATP-binding site, preventing their oxidation. The formation of ABL1 complexes with the ATP-competitive synthetic inhibitors imatinib mesylate and danusertib follows a similar mechanism and the electroactive centres of both compounds are inside the binding site preventing oxidation. Small enzyme conformational modifications were observed after interaction with danusertib. On the other hand, the natural inhibitor genistein is encountered on the outer surface of the enzyme and the electroactive centres are available for oxidation.

The electrochemical investigation of ABL1 electron-transfer reactions before and after interaction with substrates and inhibitors contributes to the development of structure–activity relationships in ligand-ABL1 kinase interactions, allows detection of ABL1 conformational modifications upon interaction with ligands and a qualitative understanding of the interaction mechanisms.

Conflict of interest

No conflict of interest.

Acknowledgements

Financial support from: Fundação para a Ciência e Tecnologia (FCT), projects PTDC/SAU-BEB/104643/2008, PTDC/DTP-FTO/0191/2012, PEst-C/EME /UI0285/2013 and CENTRO-07-0224-FEDER-002001 (MT4MOBI) (co-financed by the European Community Fund FEDER), FEDER funds through the program COMPETE – Programa Operacional Factores de Competitividade is gratefully acknowledged.

References

[1] J. Brognard, T. Hunter, Curr. Opin. Genet. Dev. 21 (2011) 4–11.
[2] A. Derouiche, C. Cousin, I. Mijakovic, Curr. Opin. Biotechnol. 23 (2012) 585–590.
[3] T.M. Pitts, S.L. Davis, S.G. Eckhardt, E.L. Bradshaw-Pierce, Pharmacol. Ther. 142 (2014) 258–269.
[4] O. Hantschel, Genes Cancer 3 (2012) 436–446.
[5] S. Medves, J.-B. Demoulin, J. Cell. Mol. Med. 16 (2012) 237–248.
[6] S. Schenone, O. Bruno, M. Radi, M. Botta, Med. Res. Rev. 31 (2010) 1–41.
[7] B. Nagar, J. Nutr. 137 (2007) 1518S–1523S.
[8] S.R. Hubbard, EMBO J. 16 (1997) 5573–5581.
[9] T. Schindler, W. Bornmann, P. Pellicena, W.T. Miller, B. Clarkson, J. Kuriyan, Science 289 (2000) 1938–1942.
[10] G. Agullo, L. Garnet-Payrustre, S. Manenti, C. Viala, C. Remesy, H. Chap, B. Payrastre, Biochem. Pharmacol. 53 (1997) 1649–1657.
[11] K. Polkowsky, A.P. Mazurek, Acta. Pol. Pharm. 57 (2000) 135–155.
[12] M. Deininger, E. Buchdunger, B.J. Druker, Blood 105 (2005) 2640–2653.
[13] S.W. Cowan-Jacob, G. Fendrich, A. Floersheimer, P. Furet, J. Liebetanz, G. Rummel, P. Rheinberger, M. Centeleghe, D. Fabbro, P.W. Manley, Acta Crystallogr. D 63 (2007) 80–93.
[14] A. Gontarewicz, T.H. Brummendorf, Recent Res. Cancer 184 (2010) 199–214.
[15] M. Modugno, E. Casale, C. Soncini, P. Rosettani, R. Colombo, R. Lupi, L. Rusconi, D. Fancelli, P. Carpinell, A.D. Cameron, A. Isacchi, J. Moll, Cancer Res. 67 (2007) 7987–7990.
[16] M. Kollareddy, P. Dzubak, D. Zheleva, M. Hajduch, Biomed. Pap. 152 (2008) 27–33.
[17] C. Naujokat, D. Fuchs, C. Berges, Biochim. Biophys. Acta 1773 (2007) 1389–1397.
[18] S. Martic, M. Labib, H.-B. Kraatz, Electrochim. Acta 56 (2011) 10676–10682.
[19] M. Mielecki, J. Wojtasik, M. Zborowska, K. Kurzatkowska, K. Grzelak, W. Dehaen, J. Radecki, H. Radecka, Electrochim. Acta 96 (2013) 147–154.
[20] V.C. Diculescu, T.A. Enache, Anal. Chim. Acta 845 (2014) 23–29.
[21] R. Gulaboski, V. Mirceski, I. Bogeski, M. Hoth, J. Solid State Electrochem. 16 (2012) 2315–2328.
[22] V.C. Diculescu, A.-M. Chiorcea-Paquim, R. Eritja, A.M. Oliveira-Brett, J. Electroanal. Chem. 656 (2011) 159–166.
[23] T.A. Enache, A.M. Oliveira-Brett, Bioelectrochemistry 89 (2013) 11–18.
[24] S.C.B. Oliveira, I.B. Santarino, A.M. Oliveira Brett, Electroanalysis 25 (2013) 1029–1034.
[25] T.A. Enache, A.M. Oliveira-Brett, Bioelectrochemistry 81 (2011) 46–52.
[26] T.A. Enache, A.M. Oliveira-Brett, J. Electroanal. Chem. 655 (2011) 9–16.
[27] T.A. Enache, A.M. Oliveira-Brett, Electroanalysis 23 (2011) 1337–1344.
[28] O.M. Popa, V.C. Diculescu, J. Electroanal. Chem. 689 (2013) 216–222.
[29] O.M. Popa, V.C. Diculescu, Electroanalysis 25 (2013) 1201–1208.
[30] O.M. Popa, V.C. Diculescu, J. Electroanal. Chem. 708 (2013) 108–115.
[31] V.C. Diculescu, M. Vivan, A.M. Oliveira Brett, Electroanalysis 18 (2006) 1800–1807.
[32] O.M. Popa, V.C. Diculescu, Electrochim. Acta 112 (2013) 486–492.
[33] J. Kyte, R. Doolittle, J. Mol. Biol. 157 (1982) 105–132.
[34] http://www.uniprot.org/uniprot/P00519.
[35] http://web.expasy.org/protscale/.
[36] J.L. Moreland, A. Gramada, O.V. Buzko, Q. Zhang, P.E. Bourne, BMC Bioinformatics 6 (2005) 21.
[37] www.rcsb.org.
[38] H.M. Berman, J. Westbrook, Z. Feng, G. Gilliland, T.N. Bhat, H. Weissig, I.N. Shindyalov, P.E. Bourne, Nucleic Acids Res. 28 (2000) 235–242.